Cell-scale dynamic recycling and cortical flow of the actin–myosin cytoskeleton for rapid cell migration

Shigehiko Yumura[1,*], Go Itoh[1,2], Yumi Kikuta[1], Takeomi Kikuchi[1], Toshiko Kitanishi-Yumura[1] and Masatsune Tsujioka[3,4]

[1]Department of Functional Molecular Biology, Graduate School of Medicine, Yamaguchi University, Yamaguchi 753-8512, Japan
[2]Institute of Development, Aging and Cancer, Tohoku University, Miyagi 980-8575, Japan
[3]Department of Biological Science, Graduate School of Science, Osaka University, 1-1 Machikaneyama, Toyonaka, Osaka 560-0043, Japan
[4]Core Research for Evolutional Science and Technology Agency, 6-2-3 Furuedai, Suita, Osaka 565-0874, Japan
*Author for correspondence (yumura@yamaguchi-u.ac.jp)

Biology Open 2, 200–209
doi: 10.1242/bio.20122899
Received 21st August 2012
Accepted 23rd October 2012

Summary

Actin and myosin II play major roles in cell migration. Whereas pseudopod extension by actin polymerization has been intensively researched, less attention has been paid to how the rest of the actin cytoskeleton such as the actin cortex contributes to cell migration. In this study, cortical actin and myosin II filaments were simultaneously observed in migrating *Dictyostelium* cells under total internal reflection fluorescence microscopy. The cortical actin and myosin II filaments remained stationary with respect to the substratum as the cells advanced. However, fluorescence recovery after photobleaching experiments and direct observation of filaments showed that they rapidly turned over. When the cells were detached from the substratum, the actin and myosin filaments displayed a vigorous retrograde flow. Thus, when the cells migrate on the substratum, the cortical cytoskeleton firmly holds the substratum to generate the motive force instead. The present studies also demonstrate how myosin II localizes to the rear region of the migrating cells. The observed dynamic turnover of actin and myosin II filaments contributes to the recycling of their subunits across the whole cell and enables rapid reorganization of the cytoskeleton.

Key words: Actin, GFP, Myosin, Retrograde flow, TIRF

Introduction

Cell migration is essential for various cellular activities, including morphogenesis, tissue repair, and the immune response. Cell migration involves coordination between protrusion at the anterior end of the cell, construction of new adhesive foci on the substratum, breakdown of old adhesive foci, and retraction of the posterior end of the cell. The migrating cell usually extends one or two large pseudopods such as lamellipods or lobopods in the anterior region. Recent studies have determined that the extension of these pseudopods results from Arp2/3-mediated actin polymerization that pushes the anterior cell membrane (Machesky and Insall, 1998; Pantaloni et al., 2001; Small et al., 2002; Pollard and Borisy, 2003; Le Clainche and Carlier, 2008). Actin filaments depolymerize at the rear edge of the pseudopod in a process mediated by ADF/cofilin proteins (Pollard and Borisy, 2003). The balance between polymerization and depolymerization keeps the breadth of the pseudopod constant. Monomeric actin is recruited at the leading edge and moves toward the rear in a ‘treadmilling’ process that does not change the breadth of the pseudopod (Wang, 1985). Simultaneously, the polymerized actin filaments themselves often flow backwards relative to the substratum as the cell advances in a process known as ‘retrograde flow’. Recent research using mammalian cells has shown that the retrograde flow of actin is driven not only by actin polymerization but also by myosin II activity (Henson et al., 1999; Ponti et al., 2004; Giannone et al., 2007; Gardel et al., 2008; Renkawitz et al., 2009).

When small beads are attached to the surface of a cell, they move toward the center or the rear of the cell (Abercrombie et al., 1970; Harris and Dunn, 1972). The beads can attach to membrane proteins, which link the beads to the actin filaments underlying the cell membrane (Forscher et al., 1992; Wang et al., 1994). The retrograde flow of actin is conspicuously evident in relatively slow-moving cells such as fibroblasts and the growth cones of neuronal cells (Wang, 1985; Okabe and Hirokawa, 1991; Lin et al., 1996), but not in fast-moving cells such as keratocytes (Theriot and Mitchison, 1991; Jay, 2000). However, this flow can be observed even in keratocytes, depending on the cell velocity (Jurado et al., 2005). This discrepancy has been explained by the ‘clutch hypothesis’, which posits that if the polymerizing actin filaments are firmly linked to the substratum through the membrane proteins at focal adhesions, they do not show retrograde flow but instead propel cell migration (Mitchison and Kirschner, 1988; Jay, 2000). Whereas numerous studies have focused on actin polymerization and turnover in the lamellipods, less attention has been paid to how the actin cytoskeleton is generated in the other regions or how it contributes to the motile machinery of the whole cell. Actin filaments are generally associated with the entire cell membrane. These filaments form a

continuous meshwork underlying the cell membrane (commonly referred to as 'cortical actin' or the 'actin cortex'), and have been shown to play important roles in maintaining the rigidity and elasticity of the cell cortex. However, it is not clear whether the actin cortex contributes to cell migration.

In the present study, we focused on the dynamics of actin and myosin II in the cortex of fast-migrating *Dictyostelium* cells. The results demonstrated that both actin and myosin II filaments in the cortex showed dynamic turnover but remained stationary with respect to the substratum as the cell advanced, suggesting a possible mechanism by which myosin II accumulates at the rear of migrating cells. When the cells were detached from the substratum, both actin and myosin II filaments vigorously flowed from the anterior to the posterior of the cells. These observations indicate that the actin cortex in migrating *Dictyostelium* cells firmly clutches the substratum and facilitates rapid cell movement. Furthermore, we propose that there is a recycling system to prevent actin and myosin II from over-accumulating in the rear.

Results

Observation of cortical actin filaments under TIRF microscopy

Actin filaments are primarily condensed in pseudopods at the anterior end of migrating *Dictyostelium* cells (Fig. 1). Actin polymerization is considered to push the anterior cell membrane, resulting in the extension of pseudopods. Actin filaments also form a thin layer of meshwork underlying the entire cell membrane (Fig. 1). To investigate the dynamics of the cortical actin meshwork during cell migration, total internal reflection fluorescence (TIRF) microscopy was employed. This technique can visualize ~100 nm in depth from the surface of the coverslip, which corresponds to the thickness of the cortex, including the cell membrane and the cortical actin meshwork (Fig. 1). In these experiments, the cells were slightly compressed by a thin agarose sheet to visualize the cortical actin clearly by TIRF microscopy. This compression was necessary because the cells sometimes adopted a more complicated three-dimensional morphology, and some parts did not attach to the substratum (Yumura et al., 1984). Under this slight compression, cells can easily migrate by extending one or more pseudopods. Fig. 2 shows typical TIRF images of a migrating cell. Actin filaments were clearly visualized by expressing GFP-ABD, i.e. a green fluorescent protein-tagged actin-binding domain of ABP120, the *Dictyostelium* filamin (Bretschneider et al., 2004). The finest filaments in the TIRF images were estimated to consist of 2–5 actin filaments by comparing them with the fluorescence intensity of single filopods, which contain bundles of 6–16 actin filaments (Bretschneider et al., 2004). Fig. 2E shows the pseudocolored superimposition of two successive images taken at an interval of 10 seconds (depicted in green and red, respectively). Most of the discernible filament bundles in the middle portion appeared yellow after superimposition, indicating

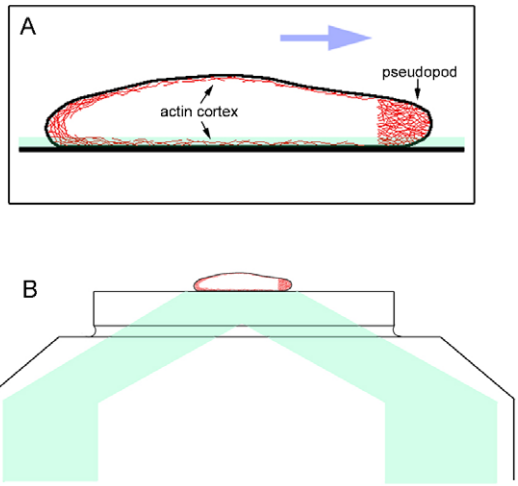

Fig. 1. Schematic of the actin cytoskeleton in a migrating *Dictyostelium* cell. (**A**) The cell contains a dense meshwork in the anterior pseudopod and a thin layer of actin meshwork (actin cortex) underlying the cell membrane (red). The average size of the cells is 15–20 μm in length and 2 μm in height. The blue arrow shows the direction of cell migration. (**B**) The TIRF microscope illuminates ~100 nm above the surface of the coverslip, which encompasses the total thickness of the ventral cortex including the cell membrane and the cortical actin meshwork. The path of illumination from the laser is depicted in pale green.

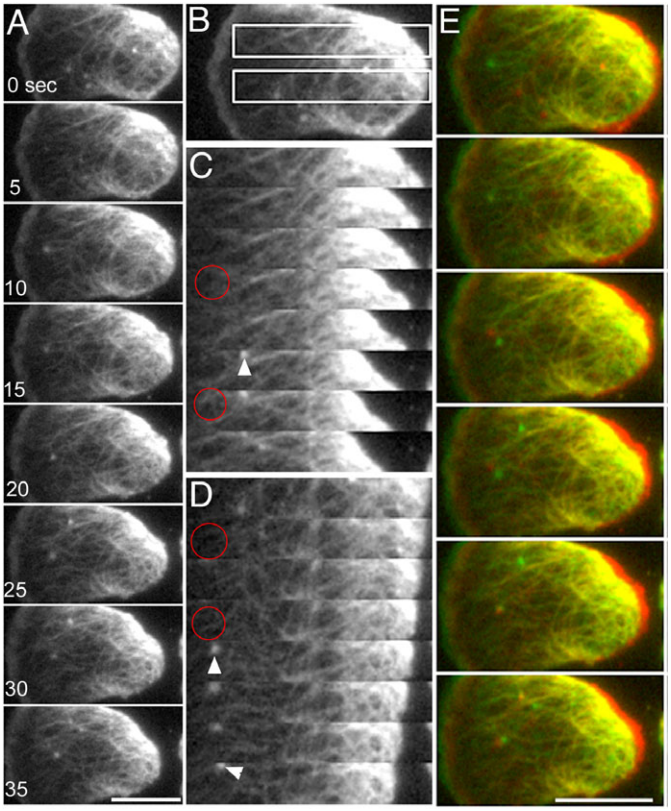

Fig. 2. TIRF microscopy of the actin cortex in a migrating cell. GFP-ABD was expressed in the cells to visualize actin filaments. Cells were slightly compressed by an agarose sheet to visualize actin filaments clearly by TIRF microscopy. (**A**) Typical TIRF images of a cell migrating toward the left. (**C**,**D**) Two kymographs corresponding to the rectangles in panel **B**. Some actin filaments were newly appeared although most were persistent (red circles indicate the appearance of the filaments). Small actin foci (arrowheads) frequently appeared and disappeared in the cortical actin network. These foci represent adhesive contacts between the cortical actin of *Dictyostelium* cells and the substratum (Yumura and Kitanishi-Yumura, 1990a; Uchida and Yumura, 2004). (**E**) Pseudocolored superimpositions of two successive images taken at an interval of 10 seconds (depicted in red and green). Most of the filaments appeared yellow, indicating that they were stationary relative to the substratum as the cell advanced. At the rearmost end of the cell, networks of actin filaments were deformed and sometimes dragged forward as the rear end advanced. Scale bars: 10 μm.

that they remained stationary relative to the substratum during the interval. At the rear of the cell, the actin filament networks were deformed, condensed and finally dragged forward due to the retraction of the rear of the cell. The two kymographs shown in Fig. 2C,D, corresponding to the rectangles depicted in Fig. 2B, demonstrate that some actin filaments were newly added (Fig. 2C,D, red circles) although most remained stationary. The enrichment in fluorescence at the rear end of the cell is likely caused by changes in the position or deformations of the actin meshwork that occurs as the cell advances and drags the rear cortex. These results indicate that the cortical actin meshwork is predominantly stationary relative to the substratum during cell migration.

Actin and myosin II rapidly turn over in the cortex

Although the above observations revealed that the cortical actin network was stationary as the cell advanced, actin filaments may themselves turn over at the subunit level. To quantitatively investigate the turnover of the cortical actin meshwork, fluorescence recovery after photobleaching (FRAP) experiments were performed by focusing only on the ventral cortex (optical section: 0.9 μm) under confocal microscopy. Filamentous structures could be observed to some extent in this domain. When a region of the cortex of a migrating cell expressing GFP-ABD was photobleached (Fig. 3A,C), the half-time of recovery was 0.62±0.12 second (n=12). During the recovery, the bleached region was stationary relative to the substratum as the cell advanced, although in many cases the fluorescence recovery occurred too rapidly relative to the cell's velocity for this to be observed. In the presence of jasplakinolide, a membrane-permeable actin-stabilizer, the half-time of recovery was significantly lengthened (1.82±0.39 seconds, n=26) (Fig. 3E,G).

FRAP experiments were also performed on cells expressing GFP-myosin II (Fig. 3B,D). Here, the half-time of recovery was 7.1±0.3 seconds (n=13), which was much slower than that of actin. The bleached regions were stationary relative to the substratum as the cell advanced. FRAP experiments were also performed in myosin II null cells expressing GFP-3ALA myosin II, in which the three phosphorylatable threonine residues of the heavy chains were replaced with alanines. This mutant myosin II can neither be phosphorylated nor disassembled into monomers. Under these conditions, the recovery of fluorescence after photobleaching became very slow, as previously shown in dividing cells (Yumura, 2001). Fig. 3F shows that the remaining fluorescent band between two bleached regions did not move relative to the substratum as the cell advanced. Interestingly, both actin in the presence of jasplakinolide and 3ALA myosin II intensely accumulated at the rear region of migrating cells (Fig. 3E,F).

The TIRF microscopy and FRAP experiments thus showed that cortical actin and myosin II filaments rapidly turn over,

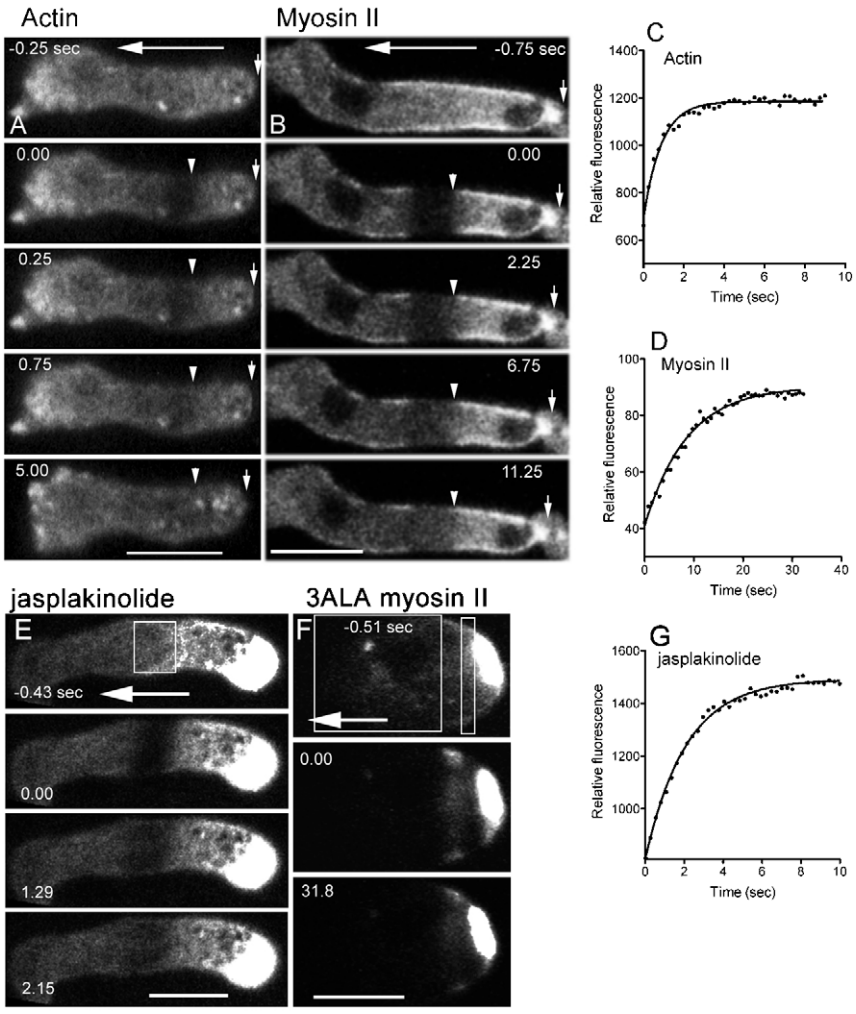

Fig. 3. Cortical actin and myosin II were stationary with respect to the substratum. The fluorescent signal in the cortex was bleached with a confocal microscope in the middle region of rapidly migrating cells expressing GFP-ABD (**A**) or GFP-myosin II (**B**) (optical section: 0.9 μm). Large arrows indicate the direction of cell migration, small arrows indicate the rear end of the cell, and arrowheads indicate the rear end of the bleached regions. The bleached regions did not move as the cells advanced.
(**E**) Photobleaching was performed on migrating cells expressing GFP-ABD in the presence of 3.5 μM jasplakinolide. The white box indicates the bleached region. Note that actin intensively accumulated at the rear region of the cell in the presence of jasplakinolide.
(**F**) Photobleaching was performed on a myosin null cell expressing GFP-3ALA myosin II. The white boxes indicate the bleached regions. Note that 3ALA myosin II intensively accumulated at the rear region. Graphs **C**,**D**,**G** show the time courses of fluorescence recovery in the bleached regions depicted in panels A,B,E, respectively. Scale bars: 10 μm.

likely exchanging with soluble subunits in the cytoplasm, although their large-scale construction seemed to be stationary.

Myosin II filaments associate and dissociate with actin filaments in the cortex

To further investigate the dynamics of individual myosin II filaments and their association with actin filaments in the cortex, GFP-ABD and mRFP-myosin II were simultaneously expressed in myosin II null cells. Fig. 4 shows TIRF microscopy of actin and myosin II in the ventral cortex. Myosin II appeared as rod-like structures with an average length of 0.6–0.7 μm (Figs 4, 5), which is comparable to the individual bipolar filaments previously identified *in vivo* and *in vitro* by immunofluorescence and immunoelectron microscopic studies (Yumura and Fukui, 1985; Yumura and Kitanishi-Yumura, 1990b). Myosin II filaments were primarily located at the rear of migrating cells, as shown previously (Yumura et al., 1984). Myosin II filaments also appeared abruptly in association with the cortical actin filaments (Fig. 4, arrows). Myosin II filaments remained stationary relative to the substratum during their association with actin filaments (Fig. 4, arrowheads), which was consistent with the results of the FRAP experiments (Fig. 3).

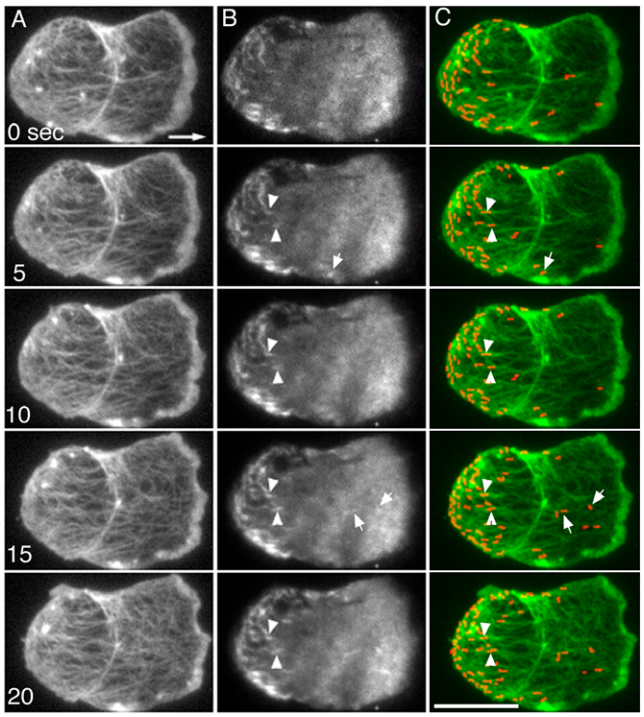

Fig. 4. Simultaneous TIRF microscopy of actin and myosin II in a migrating cell. Actin (**A**) and myosin II (**B**) filaments were simultaneously observed under TIRF microscopy. The large arrow shows the direction of cell migration. Myosin II filaments were mainly distributed at the rear of the migrating cells and associated with the actin filaments. Myosin II filaments were stationary relative to the substratum (arrowheads) as the cell advanced. Some of the filaments reached the rear end of the cell and accumulated as the cell advanced. Note that some myosin II filaments appeared *de novo* (small arrows). (**C**) Pseudocolored superimposed images of actin (green) and myosin II (red). All of the myosin II filaments appeared yellow or orange after superimposition, indicating that they were associated with actin filaments. Note that the axis of the myosin II filaments changed at the rear end of the cell; the filaments were orientated randomly or slightly parallel to the axis of cell migration at the anterior but were vertical at the rearmost end of the cell. Actin filaments also changed their orientation to the vertical axis at the rear end of the cell. These changes in orientation may reflect the contraction at the cell posterior mediated by an interaction between actin and myosin II filaments. Scale bar: 10 μm.

Interestingly, myosin II filaments also showed dynamic features. Fig. 5A shows sequential images, in which myosin II filaments appeared and then disappeared without changing position. Fig. 5B shows that the average duration of their appearance was 7.5±3.1 seconds (average±SD, n=189 filaments), which is consistent with that of myosin II filaments in dividing *Dictyostelium* cells (Yumura et al., 2008). Because the phosphorylation-deficient myosin II (3ALA) filaments appeared for much longer time (data not shown), the observed disappearance of filaments can be explained by the disassembly of filaments mediated by the heavy chain phosphorylation, as previously demonstrated (Yumura, 2001).

Fig. 5C,D presents detailed images of actin and myosin II filaments under TIRF microscopy. Myosin II filaments abruptly appeared, associated with actin filaments (red circles) and then disappeared (red squares). It is noteworthy that these myosin II filaments always associated with actin filaments.

The dorsal cortical actin cytoskeleton is linked to the ventral cytoskeleton and the substratum

Although it is difficult to observe cortical actin and myosin II filaments in the dorsal cell cortex by TIRF microscopy, it is possible to observe the cortical flow indirectly by attaching beads to the dorsal surface of the cell. When carboxylated beads or Concanavalin A-labeled beads were attached to the dorsal surface of migrating cells, they slightly fluctuated in position but essentially remained stationary relative to the substratum as the cell advanced (Fig. 6). The beads were finally collected at the rearmost end of the cell and dragged as the cell advanced (Fig. 6, 70–80 seconds). It has been shown that the beads attached in this way are linked to the dorsal cortical actin network (Forscher et al., 1992; Wang et al., 1994). The above observation is reminiscent of the results of photobleaching experiments on membrane lipids in rapidly moving leukocytes, in which the bleached lines in both the dorsal and ventral cell surfaces showed neither any forward movement nor retrograde flow (Lee et al., 1990).

Because the beads remained stationary relative to the substratum, it is plausible that the dorsal cortical actin, which is continuously linked to the ventral actin cortex, is indirectly linked to the substratum.

Rapid retrograde flow of actin and myosin II filaments when cells are detached from the substratum

The above observations indicate that both the dorsal and ventral cortical actin networks are linked to the substratum. What happens when the cells are detached from the substratum? To address this issue, we first optimized the conditions that promote cell detachment from the substratum, as described in Materials and Methods. In a buffer containing ethylenediamine tetraacetic acid (EDTA), a chelator of divalent cations, cells expressing GFP-ABD and mRFP-myosin II were almost completely detached from the substratum. The cells still extended pseudopods but could not advance. To observe their behavior under TIRF microscopy, the cells were sandwiched between a coverslip and an agarose block. Interestingly, under these conditions, actin filaments rapidly flowed from the pseudopod

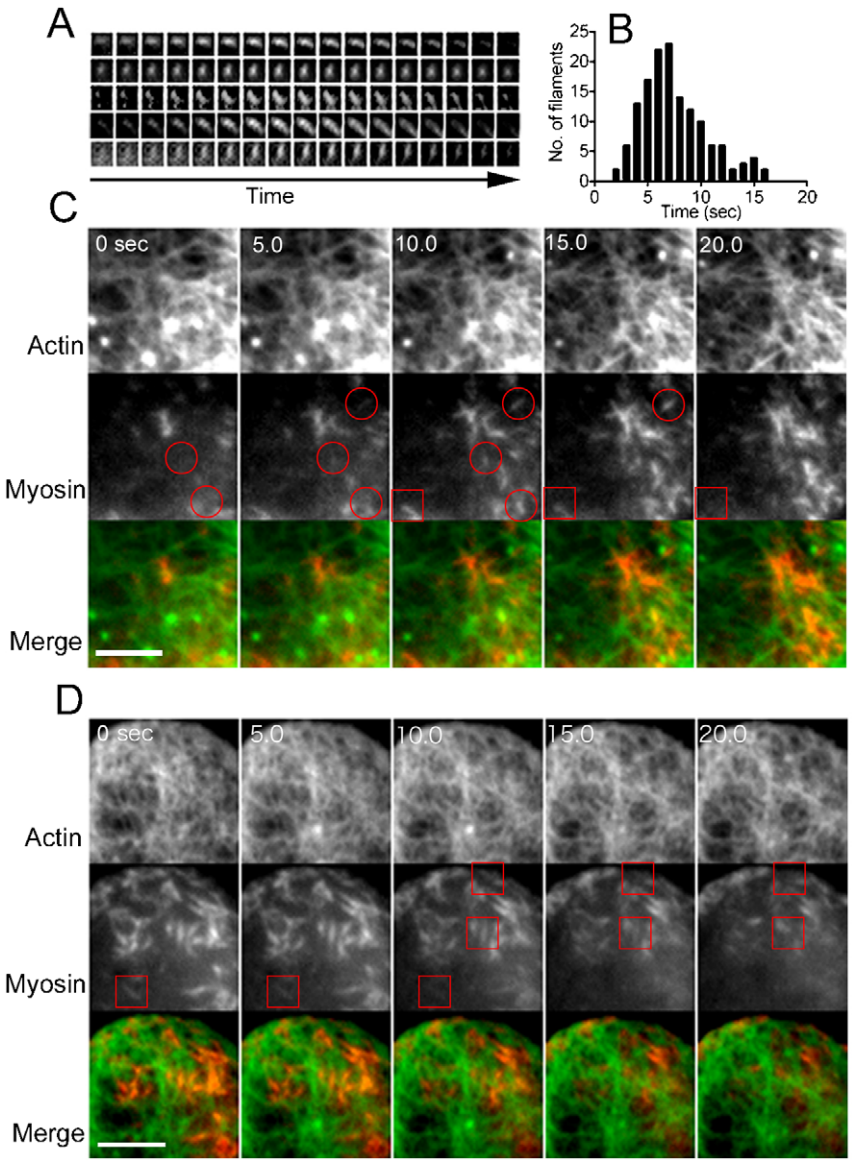

Fig. 5. Dynamics of myosin II filaments under TIRF microscopy. Myosin II filaments appeared, transiently remained in the same position, and then disappeared. Panel **A** shows five typical myosin II filaments during their appearance and disappearance (interval=0.4 second). The duration of their appearance is plotted in panel **B**, which shows that the average duration was 7.5±3.1 seconds (average±SD, n=189 filaments). Panels **C**,**D** show two typical simultaneous observations of actin and myosin II filaments in the cortex (interval=5 seconds). The colored merged images show both actin filaments (green) and myosin II filaments (red). The myosin II filaments always appeared yellow or orange due to their overlap with actin filaments. Red circles and rectangles indicate the appearance and disappearance of myosin II filaments, respectively. Note that myosin II filaments associated with cortical actin filaments and then disappeared. Scale bars: 2 μm.

toward the opposite (rear) end of the cells. Fig. 7C shows a typical kymograph of the flow (see also supplementary material Movie 1). In the presence of EDTA buffer, myosin II filaments also rapidly flowed toward the rear (Fig. 7D). The velocities of the flowing actin and myosin II filaments were identical, with an average of 0.34±0.15 μm/second (n=10).

Mutant cells deficient in both talin A and talin B, actin-binding proteins involved in cell-substratum adhesion, also cannot attach to the substratum (Tsujioka et al., 2008). These mutant cells also showed a rapid flow of actin and myosin II filaments toward the rear, with an average velocity of 0.32±0.14 μm/second (n=7) (Fig. 7F,I). The observed cortical flow is much faster than that of other types of cultured cells reported previously, e.g. 0.013 μm/second in gerbil fibroma cells, 0.075 μm/second in neuronal growth cones, and 0.027 μm/second in lung epithelial cells (Wang, 1985; Lin and Forscher, 1995; Salmon et al., 2002).

In both detached cell types, myosin II filaments frequently appeared *de novo* at the anterior region and then flowed toward the rear (supplementary material Movie 2). Interestingly, they did not disappear and actually reached the rear end of the cell. Nevertheless, they did not over-accumulate at the rear end. It seems likely that the accumulated myosin II filaments are depolymerized for recycling across the whole cell.

We tried to attach beads to the detached cells, but without success. The surface of detached cells contained convexo-concave domains. Interestingly, these convexo-concave domains also flowed toward the rear of the cell, like waves (supplementary material Movie 3). Fig. 7I,J shows the kymographs of the retrograde flow of myosin II filaments and these 'surface waves', demonstrating that their velocities were identical. Therefore, it is plausible that the observed cortical flow drives the surface waves.

Taken together, these findings indicate that the link between the actin cytoskeleton and the substratum provides a clutch or a foothold for the cells to advance on the substratum. The motive force of the observed rapid flow shifts into the motive force of cell advancement when the cells attach to the substratum and acquire a foothold.

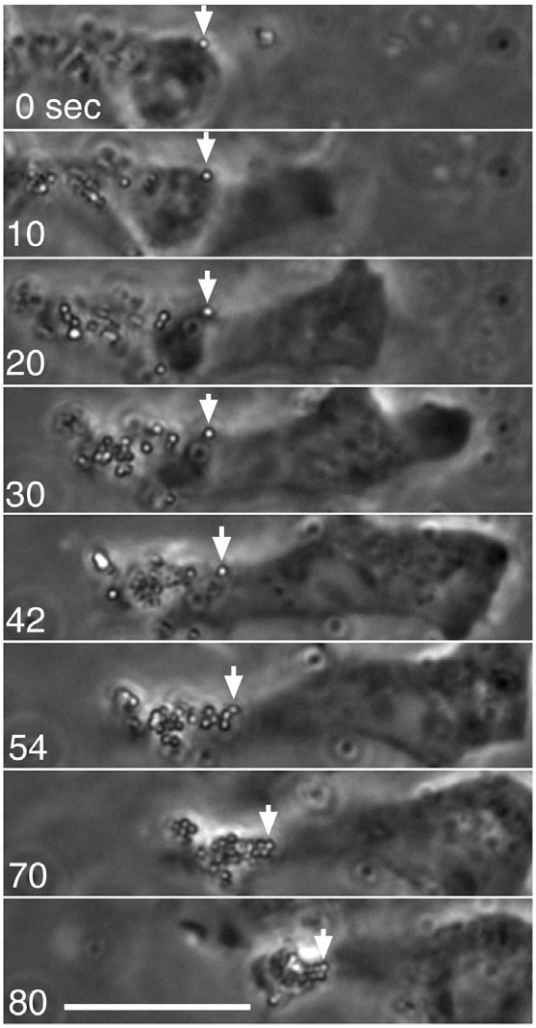

Fig. 6. Beads attached to the dorsal surface of migrating cells did not flow as the cell advanced. When carboxylated beads were attached to the dorsal surface of a migrating cell, they slightly fluctuated in position but generally remained stationary relative to the substratum as the cell advanced. As the cell advanced, the beads eventually reached the rear and were dragged, following the cell movement, and finally accumulated at the rearmost end of the cell. Note that some beads were ingested before reaching the rear and thus show different movement patterns, mediated by intracellular transport. Arrows show the positions of a single bead. See also supplementary material Movie 1. Scale bar: 10 μm.

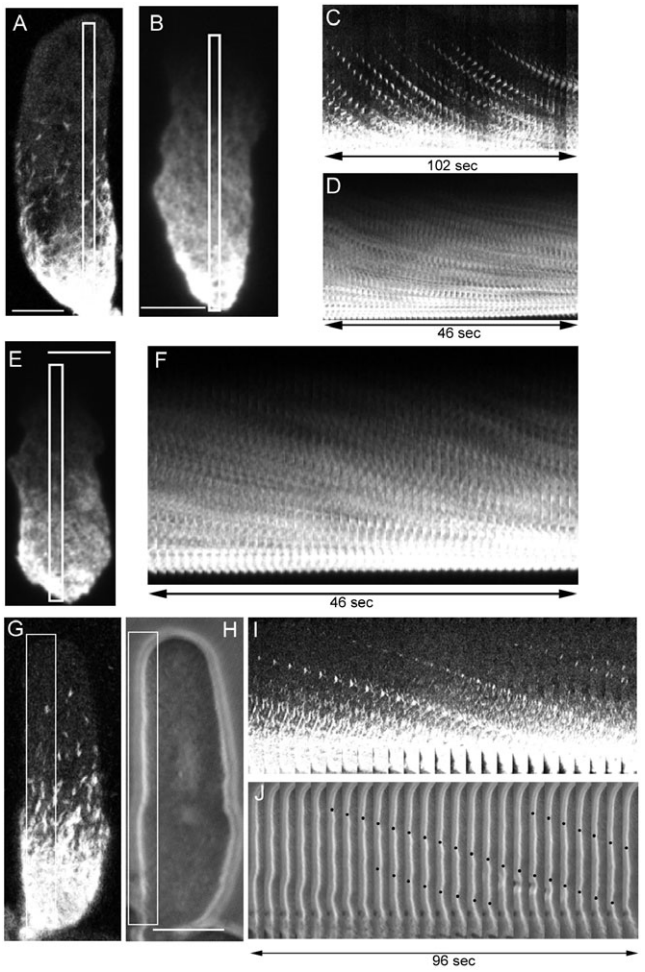

Fig. 7. Actin and myosin II filaments flow toward the rear when the cells were detached from the substratum. (**A–D**) When cells expressing GFP-myosin II (A) or GFP-ABD (B) were incubated in EDTA buffer, they completely detached from the substratum. Under these conditions, the cells were slightly compressed with an agarose block to observe the actin cortex. Panels C (actin) and D (myosin II) show kymographs corresponding to the rectangles in panels A,B, respectively. Note that actin and myosin II vigorously flowed toward the rear. The size of panels C,D was reduced to half of the original size. (**E**,**F**) Talin A/B null cells cannot attach to the substratum in normal medium. Mutant cells expressing GFP-ABD showed a vigorous flow of actin filaments toward the rear. Panel F shows a typical kymograph corresponding to the rectangle in panel E. See also supplementary material Movie 2. (**G–J**) Flow of myosin II filaments and surface waves in a talin A/B null cell. Panels I,J show typical kymographs corresponding to the rectangles in panels G,H, respectively. The size of panels I,J was reduced to half of the original size. The black dots in panel J show three waves toward the rear, which flowed at the same velocity as myosin II. See also supplementary material Movie 3. Similar surface waves were observed in detached cells in the presence of EDTA buffer (data not shown). Scale bars in panels A,B,E: 5 μm; scale bar in panel H: 10 μm.

Discussion

In the present study, cortical actin and myosin II filaments were simultaneously observed under TIRF microscopy. Importantly, all of the individual myosin II filaments were associated with cortical actin filaments. Previous experiments showed that a substantial amount of myosin II filaments dissociated from the cortex after cells were treated with latrunculin A (Yumura et al., 2008). It is now evident that myosin II filaments do not associate directly with the cell membrane but rather with cortical actin filaments, although this issue has been controversial in the past (Li et al., 1994). The present study also shows how myosin II filaments accumulate toward the rear of the migrating cells. Beads attached to the cell were stationary with respect to the substratum but finally accumulated at the rear as the cell advanced. Furthermore, lower-turnover myosin II (3ALA) and jasplakinolide-stabilized actin filaments also accumulated at the rear (Fig. 3E,F). Therefore, myosin II filaments remained stationary with respect to the substratum, resulting in their accumulation toward the rear as the cells advanced (dragging mechanism). However, we note that this is not the only strategy by which myosin II localization is controlled in the cell. In previous studies, when the cells were evenly stimulated with cAMP, a chemoattractant for *Dictyostelium*, myosin II transiently

accumulated at the cortex, without any translocation of the cell body (Yumura and Fukui, 1985; Nachmias et al., 1989). In addition, myosin II filaments abruptly appeared at the tips of pseudopods when cells change direction (Moores et al., 1996; Yumura, 1996). When a part of a cell was aspirated by a microcapillary, myosin II accumulated at the tip of the aspirated lobe (Merkel et al., 2000; Pramanik et al., 2009). These accumulations of myosin II filaments cannot be explained by the dragging mechanism. The alternative mechanism may be involved in the assembly of myosin II filaments, which is regulated by the phosphorylation of their heavy chains. There are several myosin II heavy chain kinases (MHCK): A, B, C, and D in *Dictyostelium*, all of which phosphorylate threonine residues in the tail of myosin II heavy chains, resulting in the disassembly of filaments (Betapudi et al., 2005; Yumura et al., 2005). MHCK A mainly localizes to pseudopods (Steimle et al., 2001) and MHCK C localizes to the rear of migrating cells (Nagasaki et al., 2002). MHCK A is considered to hinder myosin II filaments from localizing to pseudopods, and MHCK C may play a role in the turnover of filaments in the cortex. If MHCK A is inactivated in the pseudopod by an unknown signal promoting pseudopod retraction, myosin II will be poised to assemble in the pseudopod, thereby changing the direction of cell migration. We recently proposed an additional mechanism. Mechanically stretched actin filaments preferentially bind to the S1 fragment of myosin II, which may explain the localization of myosin II at the rear region (Uyeda et al., 2011). Therefore, multiple mechanisms are likely involved in myosin II localization.

In the present study, actin and myosin II showed remarkable dynamics, but they seemed to be stationary relative to the substratum and exhibited no flow, as depicted in Fig. 8. The meshwork of actin filaments in a pseudopod forms by recruitment of actin monomers at the leading edge and depolymerization of old filaments at the rear edge of the pseudopod. Newly polymerized filaments (Fig. 8A–C, green) push the anterior cell membrane to protrude the pseudopod, whereas old actin filaments (Fig. 8A–C, red) move backwards and disassemble when they reach the rear edge of pseudopod. At present, it is not clear whether the actin filaments in the pseudopod directly connect to the cortical actin meshwork. However, it is plausible that a part of the former connects to the latter and contributes to the traction force for cell migration. Preliminary experiments revealed that the flow of actin filaments did not cease when the detached cells were treated with blebbistatin, an inhibitor of myosin II ATPase, indicating that myosin II did not contribute to the motive force of the flow. We previously showed that there are two motive forces (pulling and pushing forces) during the biphasic migration cycle (extension and retraction phases) of *Dictyostelium* cells. These forces are highly coordinated with local adhesion to the substratum (Uchida et al., 2003). Myosin II most likely contributes to the retraction of the rear cortex, independently of the traction force revealed by the retrograde flow in the present study.

Generally, retrograde flow noticeably occurs in slowly migrating cells such as fibroblasts and neuronal growth cones (Wang, 1985; Okabe and Hirokawa, 1991; Lin et al., 1996). However, there is no or very slow retrograde flow in fast-moving cells such as keratocytes. The advance of the growth cones is inversely proportional to the retrograde flow of actin (Lin and Forscher, 1995). More recent studies have shown the interdependency of focal adhesions, actin retrograde flow, and

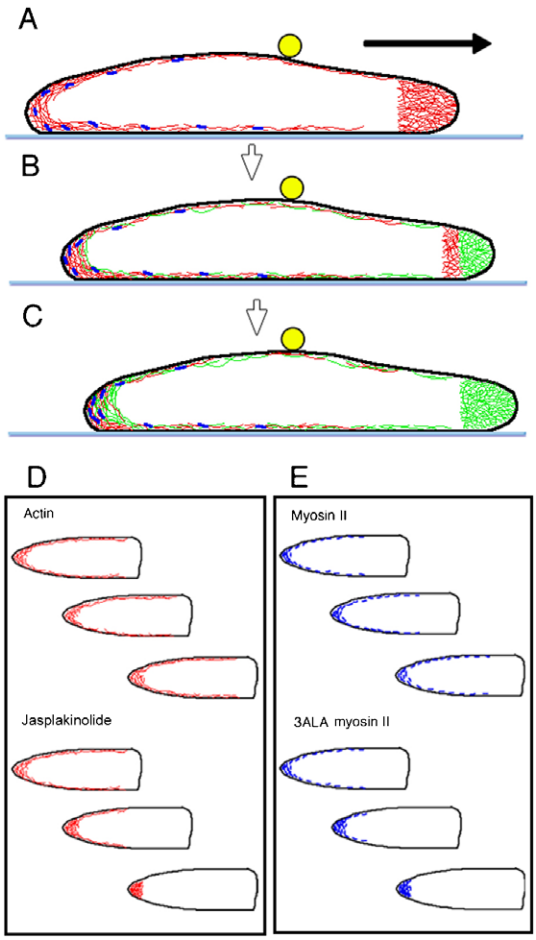

Fig. 8. A model of the dynamics of actin and myosin II during cell migration in *Dictyostelium*. Panels **A–C** show side views of a cell migrating on a substratum (light blue line). The cell contains a dense meshwork of actin filaments in the pseudopod, and a thin layer of actin meshwork underlying the cell membrane (actin cortex). The actin cortex does not move relative to the substratum. In panels A,B,C, old actin filaments are depicted in red, and new filaments are shown in green. As the cell advances, newly polymerized actin filaments push the anterior cell membrane. Simultaneously, most of the actin filaments depolymerize at the rear end of the pseudopods. At present, it is not clear but plausible that the cortical actin directly connects to part of the pseudopodal actin. Myosin II filaments (dark blue) associate with actin filaments, though some fraction of the myosin II filaments collect at the rear end of the cell in spite of their dynamic features. Beads (yellow circles) attached to the dorsal membrane are linked to the cortical actin, which forms a continuous layer with the ventral actin cortex. The beads also remain stationary relative to the substratum, but finally collect toward the rear as the cell advances. The arrow shows the direction of cell migration. (**D**) Cortical actin filaments (except those in the pseudopods) are depicted in red. The cortical actin filaments remain stationary with respect to the substratum but constantly turn over. When they are stabilized by phalloidin or jasplakinolide (lower figures), they over-accumulate at the rear as the cell advances. (**E**) Myosin II filaments also turn over. 3ALA myosin II filaments over-accumulate at the rear as the cell advances. Therefore, the turnover of actin and myosin II filaments is essential for the recycling of their subunits across the whole cell.

cell velocity on substrata of varying adhesiveness, produced by changing the amount of fibronectin coating (Gupton and Waterman-Storer, 2006; Alexandrova et al., 2008; Barnhart et al., 2011; Shao et al., 2012). The clutch hypothesis is used to explain these phenomena (Mitchison and Kirschner, 1988; Jay, 2000). Recent studies of amoeboid cells showed that actin polymerization is entirely devoted to protrusion, whereas actin

undergoes slippage and retrograde flow when the integrin–actin clutch is disengaged (Renkawitz et al., 2009). In the present study, the fact that the actin and myosin II filaments vigorously flowed backward when the cells were detached from the substratum clearly shows that the clutch hypothesis is applicable to *Dictyostelium* cells. This observation can be viewed as an explanation for the migration of a whole cell, although the retrograde flow has sometimes referred to only a limited area, such as lamellipods.

Retrograde or centripetal flow of beads attached to the cell surface has been reported in cultured cells (Abercrombie et al., 1970; Harris and Dunn, 1972). When beads are attached to dividing animal eggs or cultured cells, they flow toward the equator. In these cells, actin filaments underlying the cell membrane also flow toward the equator. Myosin II filaments flow toward the cleavage furrow in dividing *Dictyostelium* cells (Yumura, 2001; Yumura et al., 2008). This flow accompanies actual movement with respect to the substratum. Therefore, in dividing cells, cortical actin filaments may not be as firmly clutched or are often released from the clutch as the two dividing halves play at tug of war.

When a small amount of fluorescent phalloidin is introduced into a *Dictyostelium* cell, it primarily binds to the cortical actin filaments (Fukui et al., 1999). This labeled actin strongly accumulates toward the rear as the cell advances and then forms an aggregate (Fukui et al., 1999). A similar effect was observed when the cells were treated with jasplakinolide (Lee et al., 1998) (see also Fig. 3E) or when the cells expressed a GFP-labeled C-terminal fragment of talin, an actin-binding protein (Weber et al., 2002). However, in the present study, direct observations of filaments did not reveal actual flow accompanying their displacement with respect to the substratum. The accumulation of stabilized actin filaments toward the rear of migrating cells is most likely explained by a drag mechanism resulting from the forward motion of the cell. In the absence of a stabilizer, actin filaments rapidly turn over to prevent excessive accumulation of actin filaments at the rear, which facilitates recycling of actin subunits and allows for polymerization elsewhere in the cell (Fig. 8D). Recent *in vitro* and *in vivo* studies have shown that myosin II enhances actin depolymerization by cutting actin filaments, resulting in a higher rate of actin turnover (Haviv et al., 2008; Yumura et al., 2008; Stark et al., 2010; Wilson et al., 2010).

Myosin II generally localizes to the rear of migrating cells but never over-accumulates even in the face of the vigorous flow observed in detached cell. Myosin II must therefore also have a recycling system. One of these systems may depend on the turnover of actin filaments because actin filaments mediate the association of myosin II filaments with the cortex (Yumura et al., 2008). Another system seems to be independent of actin because myosin II filaments disappear even when the bound actin filaments remain, as shown in the present study.

Detachment of myosin II filaments from cortical actin requires disassembly of the myosin II filaments, mediated by the phosphorylation of the heavy chains (Yumura and Kitanishi-Yumura, 1992). This turnover occurs more slowly when the three phosphorylatable threonine residues of the heavy chains are replaced with alanines (3ALA) (Yumura, 2001). In contrast to the wild type protein, 3ALA myosin II over-accumulated at the rear of the cell during cell migration, and, importantly, these mutant cells migrated much more slowly than wild type cells (Yumura and Uyeda, 1997a). Taken together, it is highly likely that phosphorylation is involved in the turnover and recycling of myosin II across the whole cell (Fig. 8E). The rapid turnover of actin and myosin II appears crucial not only for rapid cell migration but also for the plasticity of amoeboid movements, including the reorientation of cell migration, which requires rapid reorganization of the cytoskeleton.

In conclusion, in fast-moving *Dictyostelium* cells, both actin and myosin II filaments remain stationary as the cell advances but show highly dynamic turnover. When the cells are detached from the substratum, the actin and myosin II filaments showed rapid retrograde flow. The cortical actin cytoskeletons under the ventral and dorsal surfaces of the cell are linked to each other. The cortical cytoskeleton firmly grasps the substratum and thus does not flow but rather generates a motive force against the substratum. The highly dynamic turnover of actin and myosin II is indispensable for rapid cell migration and simultaneously contributes to the recycling of their subunits across the entire cell.

Materials and Methods

Cell strains and culture

An EGFP-tagged actin-binding domain of ABP120 (GFP-ABD) and monomeric red fluorescent protein (mRFP)-tagged myosin II heavy chain (MHC) (mRFP-myosin II) were simultaneously expressed in MHC-null cells (Manstein et al., 1989; Yumura and Uyeda, 1997b). The cells expressing GFP-ABD and mRFP-myosin II were cultured in HL5 medium supplemented with 10 μg/ml G418 and 10 μg/ml Blasticidin S (Invitrogen). GFP-3ALA MHC was expressed in MHC-null cells and selected in the presence of G418 (Yumura, 2001). Cells were washed with BSS (10 mM $NaCl_2$, 10 mM KCl, 3 mM $CaCl_2$, and 2 mM MES, pH 6.3) and then incubated in the same solution for 5–7 hours before experiments. Mutant cells deficient in both talin A and talin B (talin A/B null) were cultured in HL5 medium supplemented with 10 μg/ml Blasticidin S and 50 μg/ml hygromycin B (Wako) as previously described (Tsujioka et al., 2008). GFP-ABD or GFP-MHC was expressed in the talin A/B null cells and selected in the presence of G418.

Microscopy

Cells were placed on a coverslip (18×18 mm, no.1, Matsunami Inc.) and overlaid with a thin agarose sheet as described previously (Yumura et al., 1984). The coverslip was inverted and placed over a glass slide attached to supports made of double-sided adhesive tape (5×20 mm, 0.3 mm thick). The sample was then sealed with plastic glue (Fastening Systems, USA). Cells were observed under a TIRF microscope of our own composition (Tokunaga et al., 1997; Sako et al., 2000). An inverted microscope (Olympus IX-70, Japan) was connected to an argon laser (488 nm, H210AL, National Laser Inc.) and a helium–neon laser (543 nm, LHGR-0200, Research Electro Optics Inc.) as previously described (Yumura et al., 2008). Chromatic aberration was improved by replacing all lenses with achromat lenses. The images were acquired with a cooled CCD camera (Orca ER, Hamamatsu Photonics) and processed with a computer and imaging software (IPlab, Scanalytics). To minimize photobleaching during image acquisition, the intensity of the excitation light was set at minimum. The decrease in the fluorescence intensity after each observation was less than 1–2%, and this level of excitation did not affect cell behavior or motility. Confocal microscopy and photobleaching were performed on a LSM510META microscope (Carl Zeiss) as previously described (Yumura, 2001). Briefly, the full power of the argon laser (488 nm line) was applied to a particular region of a cell. Changes in fluorescence intensity in the bleached area were monitored with respect to time after background subtraction. The time course of recovery was fitted to the equation for a single exponential rise to maximum using ImageJ software (http://rsbweb.nih.gov/ij), and the half-time recovery was calculated as previously described (Yumura, 2001).

To observe the movement of beads, cells were placed in a glass-bottomed chamber. A small amount of solution containing carboxylated beads (0.5 μm in diameter, Molecular Probes) was applied to the cells using a micropipette under a phase-contrast inverted microscope (TE300, Nikon). All images were processed and analyzed using ImageJ software.

To detach the cells from the substratum, the external solution was exchanged with an EDTA solution (10 mM NaCl, 10 mM KCl, 2 mM EDTA, 0.1 mM $MgCl_2$, and 2 mM MES, pH 6.3). After 30–60 minutes, all cells were detached from the substratum. To observe the ventral surface of the detached cells and talin A/B null cells by TIRF microscopy, the cells were settled on a glass-bottomed dish and then overlaid with a 2 mm-thick agarose block.

Acknowledgements

The authors would like to thank Drs T.Q.P. Uyeda and A. Nagasaki for sharing GFP-ABD and for helpful discussion. This research was supported by Grants-in-Aid for Scientific Research from the Japan MEXT and JSPS.

Competing Interests

The authors have no competing interests to declare.

References

Abercrombie, M., Heaysman, J. E. and Pegrum, S. M. (1970). The locomotion of fibroblasts in culture. 3. Movements of particles on the dorsal surface of the leading lamella. *Exp. Cell Res.* **62**, 389-398.

Alexandrova, A. Y., Arnold, K., Schaub, S., Vasiliev, J. M., Meister, J. J., Bershadsky, A. D. and Verkhovsky, A. B. (2008). Comparative dynamics of retrograde actin flow and focal adhesions: formation of nascent adhesions triggers transition from fast to slow flow. *PLoS ONE* **3**, e3234.

Barnhart, E. L., Lee, K. C., Keren, K., Mogilner, A. and Theriot, J. A. (2011). An adhesion-dependent switch between mechanisms that determine motile cell shape. *PLoS Biol.* **9**, e1001059.

Betapudi, V., Mason, C., Licate, L. and Egelhoff, T. T. (2005). Identification and characterization of a novel α-kinase with a von Willebrand factor A-like motif localized to the contractile vacuole and Golgi complex in *Dictyostelium discoideum*. *Mol. Biol. Cell* **16**, 2248-2262.

Bretschneider, T., Diez, S., Anderson, K., Heuser, J., Clarke, M., Müller-Taubenberger, A., Köhler, J. and Gerisch, G. (2004). Dynamic actin patterns and Arp2/3 assembly at the substrate-attached surface of motile cells. *Curr. Biol.* **14**, 1-10.

Forscher, P., Lin, C. H. and Thompson, C. (1992). Novel form of growth cone motility involving site-directed actin filament assembly. *Nature* **357**, 515-518.

Fukui, Y., Kitanishi-Yumura, T. and Yumura, S. (1999). Myosin II-independent F-actin flow contributes to cell locomotion in *Dictyostelium*. *J. Cell Sci.* **112**, 877-886.

Gardel, M. L., Sabass, B., Ji, L., Danuser, G., Schwarz, U. S. and Waterman, C. M. (2008). Traction stress in focal adhesions correlates biphasically with actin retrograde flow speed. *J. Cell Biol.* **183**, 999-1005.

Giannone, G., Dubin-Thaler, B. J., Rossier, O., Cai, Y., Chaga, O., Jiang, G., Beaver, W., Döbereiner, H. G., Freund, Y., Borisy, G. et al. (2007). Lamellipodial actin mechanically links myosin activity with adhesion-site formation. *Cell* **128**, 561-575.

Gupton, S. L. and Waterman-Storer, C. M. (2006). Spatiotemporal feedback between actomyosin and focal-adhesion systems optimizes rapid cell migration. *Cell* **125**, 1361-1374.

Harris, A. and Dunn, G. (1972). Centripetal transport of attached particles on both surfaces of moving fibroblasts. *Exp. Cell Res.* **73**, 519-523.

Haviv, L., Gillo, D., Backouche, F. and Bernheim-Groswasser, A. (2008). A cytoskeletal demolition worker: myosin II acts as an actin depolymerization agent. *J. Mol. Biol.* **375**, 325-330.

Henson, J. H., Svitkina, T. M., Burns, A. R., Hughes, H. E., MacPartland, K. J., Nazarian, R. and Borisy, G. G. (1999). Two components of actin-based retrograde flow in sea urchin coelomocytes. *Mol. Biol. Cell* **10**, 4075-4090.

Jay, D. G. (2000). The clutch hypothesis revisited: ascribing the roles of actin-associated proteins in filopodial protrusion in the nerve growth cone. *J. Neurobiol.* **44**, 114-125.

Jurado, C., Haserick, J. R. and Lee, J. (2005). Slipping or gripping? Fluorescent speckle microscopy in fish keratocytes reveals two different mechanisms for generating a retrograde flow of actin. *Mol. Biol. Cell* **16**, 507-518.

Le Clainche, C. and Carlier, M. F. (2008). Regulation of actin assembly associated with protrusion and adhesion in cell migration. *Physiol. Rev.* **88**, 489-513.

Lee, J., Gustafsson, M., Magnusson, K. E. and Jacobson, K. (1990). The direction of membrane lipid flow in locomoting polymorphonuclear leukocytes. *Science* **247**, 1229-1233.

Lee, E., Shelden, E. A. and Knecht, D. A. (1998). Formation of F-actin aggregates in cells treated with actin stabilizing drugs. *Cell Motil. Cytoskeleton* **39**, 122-133.

Li, D., Miller, M. and Chantler, P. D. (1994). Association of a cellular myosin II with anionic phospholipids and the neuronal plasma membrane. *Proc. Natl. Acad. Sci. USA* **91**, 853-857.

Lin, C. H. and Forscher, P. (1995). Growth cone advance is inversely proportional to retrograde F-actin flow. *Neuron* **14**, 763-771.

Lin, C. H., Espreafico, E. M., Mooseker, M. S. and Forscher, P. (1996). Myosin drives retrograde F-actin flow in neuronal growth cones. *Neuron* **16**, 769-782.

Machesky, L. M. and Insall, R. H. (1998). Scar1 and the related Wiskott-Aldrich syndrome protein, WASP, regulate the actin cytoskeleton through the Arp2/3 complex. *Curr. Biol.* **8**, 1347-1356.

Manstein, D. J., Titus, M. A., De Lozanne, A. and Spudich, J. A. (1989). Gene replacement in Dictyostelium: generation of myosin null mutants. *EMBO J.* **8**, 923-932.

Merkel, R., Simson, R., Simson, D. A., Hohenadl, M., Boulbitch, A., Wallraff, E. and Sackmann, E. (2000). A micromechanic study of cell polarity and plasma membrane cell body coupling in *Dictyostelium*. *Biophys. J.* **79**, 707-719.

Mitchison, T. and Kirschner, M. (1988). Cytoskeletal dynamics and nerve growth. *Neuron* **1**, 761-772.

Moores, S. L., Sabry, J. H. and Spudich, J. A. (1996). Myosin dynamics in live Dictyostelium cells. *Proc. Natl. Acad. Sci. USA* **93**, 443-446.

Nachmias, V. T., Fukui, Y. and Spudich, J. A. (1989). Chemoattractant-elicited translocation of myosin in motile *Dictyostelium*. *Cell Motil. Cytoskeleton* **13**, 158-169.

Nagasaki, A., Itoh, G., Yumura, S. and Uyeda, T. Q. (2002). Novel myosin heavy chain kinase involved in disassembly of myosin II filaments and efficient cleavage in mitotic *Dictyostelium* cells. *Mol. Biol. Cell* **13**, 4333-4342.

Okabe, S. and Hirokawa, N. (1991). Actin dynamics in growth cones. *J. Neurosci.* **11**, 1918-1929.

Pantaloni, D., Le Clainche, C. and Carlier, M. F. (2001). Mechanism of actin-based motility. *Science* **292**, 1502-1506.

Pollard, T. D. and Borisy, G. G. (2003). Cellular motility driven by assembly and disassembly of actin filaments. *Cell* **112**, 453-465.

Ponti, A., Machacek, M., Gupton, S. L., Waterman-Storer, C. M. and Danuser, G. (2004). Two distinct actin networks drive the protrusion of migrating cells. *Science* **305**, 1782-1786.

Pramanik, M. K., Iijima, M., Iwadate, Y. and Yumura, S. (2009). PTEN is a mechanosensing signal transducer for myosin II localization in *Dictyostelium* cells. *Genes Cells* **14**, 821-834.

Renkawitz, J., Schumann, K., Weber, M., Lämmermann, T., Pflicke, H., Piel, M., Polleux, J., Spatz, J. P. and Sixt, M. (2009). Adaptive force transmission in amoeboid cell migration. *Nat. Cell Biol.* **11**, 1438-1443.

Sako, Y., Minoghchi, S. and Yanagida, T. (2000). Single-molecule imaging of EGFR signalling on the surface of living cells. *Nat. Cell Biol.* **2**, 168-172.

Salmon, W. C., Adams, M. C. and Waterman-Storer, C. M. (2002). Dual-wavelength fluorescent speckle microscopy reveals coupling of microtubule and actin movements in migrating cells. *J. Cell Biol.* **158**, 31-37.

Shao, D., Levine, H. and Rappel, W. J. (2012). Coupling actin flow, adhesion, and morphology in a computational cell motility model. *Proc. Natl. Acad. Sci. USA* **109**, 6851-6856.

Small, J. V., Stradal, T., Vignal, E. and Rottner, K. (2002). The lamellipodium: where motility begins. *Trends Cell Biol.* **12**, 112-120.

Stark, B. C., Sladewski, T. E., Pollard, L. W. and Lord, M. (2010). Tropomyosin and myosin-II cellular levels promote actomyosin ring assembly in fission yeast. *Mol. Biol. Cell* **21**, 989-1000.

Steimle, P. A., Yumura, S., Côté, G. P., Medley, Q. G., Polyakov, M. V., Leppert, B. and Egelhoff, T. T. (2001). Recruitment of a myosin heavy chain kinase to actin-rich protrusions in *Dictyostelium*. *Curr. Biol.* **11**, 708-713.

Theriot, J. A. and Mitchison, T. J. (1991). Actin microfilament dynamics in locomoting cells. *Nature* **352**, 126-131.

Tokunaga, M., Kitamura, K., Saito, K., Iwane, A. H. and Yanagida, T. (1997). Single molecule imaging of fluorophores and enzymatic reactions achieved by objective-type total internal reflection fluorescence microscopy. *Biochem. Biophys. Res. Commun.* **235**, 47-53.

Tsujioka, M., Yoshida, K., Nagasaki, A., Yonemura, S., Müller-Taubenberger, A. and Uyeda, T. Q. (2008). Overlapping functions of the two talin homologues in *Dictyostelium*. *Eukaryot. Cell* **7**, 906-916.

Uchida, K. S. K., Kitanishi-Yumura, T. and Yumura, S. (2003). Myosin II contributes to the posterior contraction and the anterior extension during the retraction phase in migrating *Dictyostelium* cells. *J. Cell Sci.* **116**, 51-60.

Uchida, K. S. and Yumura, S. (2004). Dynamics of novel feet of Dictyostelium cells during migration. *J. Cell Sci.* **117**, 1443-1455.

Uyeda, T. Q. P., Iwadate, Y., Umeki, N., Nagasaki, A. and Yumura, S. (2011). Stretching actin filaments within cells enhances their affinity for the myosin II motor domain. *PLoS One* **6**, e26200.

Wang, Y. L. (1985). Exchange of actin subunits at the leading edge of living fibroblasts: possible role of treadmilling. *J. Cell Biol.* **101**, 597-602.

Wang, Y. L., Silverman, J. D. and Cao, L. G. (1994). Single particle tracking of surface receptor movement during cell division. *J. Cell Biol.* **127**, 963-971.

Weber, I., Niewöhner, J., Du, A., Röhrig, U. and Gerisch, G. (2002). A talin fragment as an actin trap visualizing actin flow in chemotaxis, endocytosis, and cytokinesis. *Cell Motil. Cytoskeleton* **53**, 136-149.

Wilson, C. A., Tsuchida, M. A., Allen, G. M., Barnhart, E. L., Applegate, K. T., Yam, P. T., Ji, L., Keren, K., Danuser, G. and Theriot, J. A. (2010). Myosin II contributes to cell-scale actin network treadmilling through network disassembly. *Nature* **465**, 373-377.

Yumura, S. (1996). Rapid redistribution of myosin II in living *Dictyostelium* amoebae, as revealed by fluorescent probes introduced by electroporation. *Protoplasma* **192**, 217-227.

Yumura, S. (2001). Myosin II dynamics and cortical flow during contractile ring formation in *Dictyostelium* cells. *J. Cell Biol.* **154**, 137-146.

Yumura, S. and Fukui, Y. (1985). Reversible cyclic AMP-dependent change in distribution of myosin thick filaments in *Dictyostelium*. *Nature* **314**, 194-196.

Yumura, S. and Kitanishi-Yumura, T. (1990a). Fluorescence-mediated visualization of actin and myosin filaments in the contractile membrane-cytoskeleton complex of *Dictyostelium discoideum*. *Cell Struct. Funct.* **15**, 355-364.

Yumura, S. and Kitanishi-Yumura, T. (1990b). Immunoelectron microscopic studies of the ultrastructure of myosin filaments in *Dictyostelium discoideum*. *Cell Struct. Funct.* **15**, 343-354.

Yumura, S. and Kitanishi-Yumura, T. (1992). Release of myosin II from the membrane-cytoskeleton of Dictyostelium discoideum mediated by heavy-chain phosphorylation at the foci within the cortical actin network. *J. Cell Biol.* **117**, 1231-1239.

Yumura, S. and Uyeda, T. Q. (1997a). Myosin II can be localized to the cleavage furrow and to the posterior region of *Dictyostelium* amoebae without control by phosphorylation of myosin heavy and light chains. *Cell Motil. Cytoskeleton* **36**, 313-322.

Yumura, S. and Uyeda, T. Q. (1997b). Transport of myosin II to the equatorial region without its own motor activity in mitotic *Dictyostelium* cells. *Mol. Biol. Cell* **8**, 2089-2099.

Yumura, S., Mori, H. and Fukui, Y. (1984). Localization of actin and myosin for the study of ameboid movement in Dictyostelium using improved immunofluorescence. *J. Cell Biol.* **99**, 894-899.

Yumura, S., Yoshida, M., Betapudi, V., Licate, L. S., Iwadate, Y., Nagasaki, A., Uyeda, T. Q. and Egelhoff, T. T. (2005). Multiple myosin II heavy chain kinases: roles in filament assembly control and proper cytokinesis in *Dictyostelium*. *Mol. Biol. Cell* **16**, 4256-4266.

Yumura, S., Ueda, M., Sako, Y., Kitanishi-Yumura, T. and Yanagida, T. (2008). Multiple mechanisms for accumulation of myosin II filaments at the equator during cytokinesis. *Traffic* **9**, 2089-2099.